Finite element analysis of the phase transformation effect in residual stresses generated by quenching in notched steel cylinders

E P Silva[1], P M C L Pacheco[2], and M A Savi[3]*

[1]Truck and Bus Development, Volkswagen South America, Rio de Janeiro, Brazil

[2]Centro Federal de Educação Tecnológica do Rio de Janeiro, Celso Suckow da Fonseca, CEFET/RJ, Rio de Janeiro, Brazil

[3]COPPE–Department of Mechanical Engineering, Universidade Federal do Rio de Janeiro, Rio de Janeiro, Brazil

The MS was received on 17 February 2004 and was accepted after revision for publication on 14 September 2004.

DOI: 10.1243/030932405X7755

Abstract: The determination of residual stresses is an important task in the analysis of the quenching process. Nevertheless, because of the complexity of the phenomenon, many simplifications are usually adopted in the prediction of these stresses for engineering purposes. One of these simplifications is the effect of phase transformation. Many studies analyse residual stresses generated by the quenching process considering a thermoelastoplastic approach, neglecting phase transformation. The present study analyses the effect of austenite–martensite phase transformation during quenching in the determination of residual stresses, comparing two different models: complete (thermoelastoplastic model with austenite–martensite phase transformation) and without phase transformation (thermoelastoplastic model without phase transformation). The finite element method is employed for spatial discretization together with a constitutive model that represents the thermomechanical behaviour of the quenching process. Progressive induction hardening of steel cylinders with semicircular notches is of concern. Numerical simulations show situations where great discrepancies are introduced in the predicted residual stresses if phase transformation is neglected.

Keywords: quenching, phase transformation, thermomechanical coupling, modelling, finite element

1 INTRODUCTION

Considerable residual stresses may arise during the quenching process and, therefore, their prediction is an important task [**1–5**]. Since phenomenological aspects of quenching involve couplings between different physical phenomena, their description is unusually complex. Moreover, engineering purposes usually introduce many simplifications in order to predict the residual stresses generated during quenching. Neglecting the phase transformations is one of these simplifications in the modelling of the quenching process.

**Corresponding author: COPPE–Department of Mechanical Engineering, Universidade Federal do Rio de Janeiro, Centro de Tecnologia, G-204, PO Box 68.503, 21.945.970 Rio de Janeiro, RJ, Brazil; email: savi@ufrj.br*

Sen *et al.* [**5**] considered steel cylinders without phase transformations. Other authors analysed simple geometries incorporating the effect of phase transformations [**6–9**]. There are also some other complex aspects related to quenching that could be incorporated in the modelling of this process. For example, the heat generated during phase transformation, which is usually treated by considering the latent heat associated with phase transformation [**2**, **10–12**], can be cited. Meanwhile, other coupling terms in the energy equation related to other phenomena such as plastic strain or hardening are not usually treated in the literature and their analysis is an important topic to be investigated [**13**].

The present contribution concerns the importance of phase transformation in the analysis of residual stresses generated by the quenching process. On this basis, simulations of two different models are carried

out: complete (thermoelastoplastic model with austenite–martensite phase transformation) and without phase transformation (thermoelastoplastic model without phase transformation). The finite element method associated with a constitutive model proposed by Pacheco *et al.* [**14**, **15**] and Silva *et al.* [**13**] is considered. The constitutive model describes the thermomechanical behaviour related to the quenching process considering different phenomenological phenomena such as plasticity with kinematic hardening, thermal expansion, the austenite–martensite phase transformation and some related aspects associated with this phase transformation such as the volumetric expansion and the transformation plasticity. This anisothermal model is formulated within the framework of continuum mechanics and the thermodynamics of irreversible processes and captures the general behaviour of quenching [**13–15**]. Numerical procedures described by Silva [**16**] are employed in order to deal with non-linearities of the formulation.

In this contribution, as an application of the general procedure, progressive induction hardening of steel cylinder bodies is analysed. Since mechanical components usually have geometric discontinuities that promote local perturbations in the distribution of variables, it is important to consider this type of perturbation in the analysis. Here, this perturbation is examined by introducing a semicircular notch in the steel cylinder. Numerical simulations show situations where great discrepancies are introduced in the predicted residual stresses neglecting phase transformation.

2 CONSTITUTIVE MODEL

This contribution describes the quenching process with the aid of a constitutive model presented by Pacheco *et al.* [**14**, **15**] and Silva *et al.* [**13**]. This model is formulated within the framework of continuum mechanics and the thermodynamics of irreversible processes. Here, a brief description of this model is presented and a detailed explanation may be found in references [**13**] to [**16**]. Therefore, considering that ε_{ij} is the total strain, T the temperature, $\varepsilon^{\mathrm{p}}_{ij}$ the plastic strain, β the volumetric fraction of the martensitic phase, and α_{ij} a variable related to kinematic hardening, and denoting σ_{ij} as the stress tensor component, the constitutive relation may be written as

$$\begin{aligned}\sigma_{ij} = {} & \Phi_{ijpq}E_{pqkl}[\varepsilon_{kl} - \varepsilon^{\mathrm{p}}_{kl} - \alpha_T(T-T_0)\delta_{kl} + \gamma\beta\delta_{kl}] \\ & + \Phi_{ijpq}E_{pqkk}[\tfrac{1}{2}\kappa\beta(2-\beta)] \\ & \times \frac{\Phi_{aaef}E_{efrs}\{\varepsilon_{rs} - \varepsilon^{\mathrm{p}}_{rs} - [\alpha_T(T-T_0)+\gamma\beta]\delta_{rs}\}}{1 - \Phi_{bbcd}E_{cdgg}[\tfrac{1}{2}\kappa\beta(2-\beta)]}\end{aligned} \tag{1}$$

where E_{ijkl} is associated with components of the elastic tensor, Φ_{ijpq} is an auxiliary tensor defined as the inverse of C_{ijpq} according to

$$C_{ijpq} = \delta_{pi}\delta_{qj} + \tfrac{3}{2}E_{ijpq}\kappa\beta(2-\beta) \tag{2}$$

and δ_{ij} is the Kronecker delta. The expression for the constitutive equation is obtained assuming an elastic strain with the form

$$\begin{aligned}\varepsilon^{\mathrm{e}}_{ij} = {} & \varepsilon_{ij} - \varepsilon^{\mathrm{p}}_{ij} - \alpha_T(T-T_0)\delta_{ij} - \gamma\beta\delta_{ij} \\ & - \tfrac{3}{2}\kappa\sigma^{\mathrm{d}}_{ij}\beta(2-\beta)\end{aligned} \tag{3}$$

Observing the right-hand side of the equation, the third term $\alpha_T(T-T_0)\delta_{ij}$ is associated with thermal expansion. The parameter α_T is the coefficient of linear thermal expansion and T_0 is a reference temperature. The fourth term $\gamma\beta\delta_{ij}$ is related to volumetric expansion associated with phase transformation from austenite to martensite. Therefore, when part of a material experiences phase transformation, there is an increment of volumetric strain, proportional to γ, a material property related to the total expansion associated with martensitic transformation. Finally, the last term $\frac{3}{2}\kappa\sigma^{\mathrm{d}}_{ij}\beta(2-\beta)$ is denoted as transformation-induced plasticity strain, being the result of several physical mechanisms [**1**, **4**]. This behaviour is related to localized plastic strain promoted by the martensitic transformation. In this term, the deviatoric stress component is defined by $\sigma^{\mathrm{d}}_{ij} = \sigma_{ij} - \delta_{ij}(\sigma_{kk}/3)$. Moreover, κ is a material parameter. It should be emphasized that this strain may be related to stress states that are inside the yield surface.

The evolution of internal variables is governed by the equations

$$\dot{\varepsilon}^{\mathrm{p}}_{ij} = \lambda\,\mathrm{sgn}(\sigma_{ij} - H_{ijkl}\alpha_{kl}) \tag{4}$$

$$\dot{\alpha}_{ij} = \dot{\varepsilon}^{\mathrm{p}}_{ij} \tag{5}$$

$$\dot{\beta} = \varsigma_{\mathrm{A}\to\mathrm{M}}k\dot{T}(M_{\mathrm{s}} - T)\exp[-k(M_{\mathrm{s}} - T)] \tag{6}$$

where $\mathrm{sgn}(x) = x/|x|$ and λ is the plastic multiplier from the classical theory of plasticity. The term $H_{ijkl}\alpha_{kl} = X_{ij}$ is related to the kinematic hardening, where H_{ijkl} is the kinematic hardening modulus tensor. Phase transformation is described by the equation proposed by Koistinen and Marburger [**13**] to express the kinetics of phase transformation from austenite to martensite. In this expression, k is a material constant and M_{s} is the temperature at which martensite starts to form in the stress-free state. Moreover, the following expression is used in order to impose proper conditions on the phase transformation

$$\varsigma_{\mathrm{A}\to\mathrm{M}}(\dot{T}, T) = \Gamma(|\dot{T}| - rM_{\mathrm{s}})\Gamma(M_{\mathrm{s}} - T)\Gamma(T - M_{\mathrm{f}}) \tag{7}$$

where rM_s is the critical cooling rate for the martensite formation, defined from the continuous cooling transformation diagram, and $\dot{T}$ is the cooling rate. Moreover, $\Gamma(x)$ is the Heaviside function. The von Mises criterion is expressed by [**13**]

$$f(\sigma_{ij}, \alpha_{ij}) = [\tfrac{3}{2}(\sigma_{ij}^{\mathrm{d}} - X_{ij}^{\mathrm{d}})(\sigma_{ij}^{\mathrm{d}} - X_{ij}^{\mathrm{d}})]^{1/2} - \sigma_{\mathrm{Y}} \leqslant 0 \quad (8)$$

where σ_{Y} is the yield stress and X_{ij}^{d} is the deviatoric part of X_{ij}, the kinematic hardening tensor, defined as

$$X_{ij}^{\mathrm{d}} = X_{ij} - \delta_{ij}\frac{X_{kk}}{3} \quad (9)$$

The description of thermal problem assumes the classical energy equation

$$\frac{\partial}{\partial x_i}\left(\Lambda\frac{\partial T}{\partial x_i}\right) - \rho c\dot{T} = 0 \quad (10)$$

for rigid bodies, where Λ is the coefficient of thermal conductivity, ρ is the density, and c is the specific heat. Note that terms related to thermomechanical coupling are neglected [**13**].

These expressions provide a complete set of equations that describes the thermomechanical behaviour of solids during the quenching process. Note that it is a non-linear set and proper numerical procedures are necessary for its solution.

3 FINITE ELEMENT MODEL

In order to deal with the non-linearities of the formulation, an iterative numerical procedure is proposed on the basis of the operator split technique [**17**]. With this assumption, coupled governing equations are solved from four uncoupled problems, where classical numerical methods can be employed: thermal, phase transformation, thermoelastic and elastoplastic. In this article, the classical finite element method is employed to perform spatial discretization of governing equations. Therefore, the following moduli are considered.

1. *Thermal problem.* This consists of the conduction problem with convection. Material properties depend on temperature and, therefore, the problem is governed by non-linear parabolic equations. The classical finite element method is employed for spatial discretization while the Crank–Nicolson method is used for time discretization [**18–20**].
2. *Phase transformation problem.* The volumetric fraction of the martensitic phase is determined in this problem. Evolution equations are integrated from a simple implicit Euler method [**14**, **15**, **21**, **22**].
3. *Thermoelastic problem.* Stress and displacement fields are evaluated from temperature distribution. The classical finite element method is employed for spatial discretization [**20**].
4. *Elastoplastic problem.* Stress and strain fields are determined by considering the plastic strain evolution in the process. Numerical solution is based on the classical return mapping algorithm [**23**, **24**].

As an application of the general procedure, axisymmetric triangular elements are adopted for all finite element moduli, considering classical shape functions [**20**]. Also, the original three-dimensional constitutive model is reduced to a simplified version in order to describe the quenching process in steel cylinders. With this assumption, heat transfer analysis may be reduced to a two-dimensional problem and, for the stress components, only radial r, tangential θ, and axial z components need to be considered together with shear components rz. In brief, it is important to note that tensor quantities may be replaced by scalar or vector quantities. As examples, E_{ijkl} may be replaced by E, H_{ijkl} may be replaced by H, and the non-vanishing components of σ_{ij} are σ_r, σ_θ, σ_z, and σ_{rz}.

4 NUMERICAL SIMULATIONS

In order to analyse the effect of phase transformation during the quenching process, numerical investigations are carried out by simulating a progressive induction (PI) hardening. PI hardening is a heat treatment process that is achieved by moving a workpiece at a constant speed through a coil and a cooling ring. A hard surface layer with high compressive residual stresses, combined with a tough core with tensile residual stresses, is usually obtained.

This article considers PI hardening simulations in a long cylindrical SAE 4140H steel bar. Material parameters for numerical simulation are presented in Table 1. Other parameters depend on temperature and are interpolated from experimental data to give (in SI units) [**13–16**, **25–29**]

Table 1 Material parameters (SAE 4140H)

k	$1.100 \times 10^{-2}\,\mathrm{K}^{-1}$
κ	$5.200 \times 10^{-11}\,\mathrm{Pa}^{-1}$
M_s	748 K
M_f	573 K
γ	1.110×10^{-2}
ρ	$7.800 \times 10^{3}\,\mathrm{kg/m}^3$

$$E = E_{\mathrm{A}}(1-\beta) + E_{\mathrm{M}}\beta \begin{cases} E_{\mathrm{A}} = 1.985 \times 10^{11} - 4.462 \times 10^{7} T - 9.909 \times 10^{4} T^{2} - 2.059 T^{3} \\ E_{\mathrm{M}} = 2.145 \times 10^{11} - 3.097 \times 10^{7} T - 9.208 \times 10^{4} T^{2} - 2.797 T^{3} \end{cases} \tag{11}$$

$$H = \begin{cases} 2.092 \times 10^{8} + 3.833 \times 10^{7} T - 3.459 \times 10^{4} T^{2}, & \text{if } T \leqslant 723\,\mathrm{K} \\ 2.259 \times 10^{11} - 2.988 \times 10^{8} T, & \text{if } 723\,\mathrm{K} < T \leqslant 748\,\mathrm{K} \\ 5.064 \times 10^{9} - 3.492 \times 10^{6} T, & \text{if } T > 748\,\mathrm{K} \end{cases} \tag{12}$$

$$\sigma_Y = \begin{cases} 7.520 \times 10^{8} + 2.370 \times 10^{5} T - 5.995 \times 10^{2} T^{2}, & \text{if } T \leqslant 723\,\mathrm{K} \\ 1.598 \times 10^{10} - 2.126 \times 10^{7} T, & \text{if } 723\,\mathrm{K} < T \leqslant 748\,\mathrm{K} \\ 1.595 \times 10^{8} - 1.094 \times 10^{5} T, & \text{if } T > 748\,\mathrm{K} \end{cases} \tag{13}$$

$$\alpha_T = \begin{cases} 1.115 \times 10^{-5} + 1.918 \times 10^{-8} T - 8.798 \times 10^{-11} T^{2} + 2.043 \times 10^{-13} T^{3}, & \text{if } T \leqslant 748\,\mathrm{K} \\ 2.230 \times 10^{-5}, & \text{if } T > 748\,\mathrm{K} \end{cases} \tag{14}$$

$$c = 2.159 \times 10^{2} + 0.548 T \tag{15}$$

$$\Lambda = 5.223 + 1.318 \times 10^{-2} T \tag{16}$$

The heat transfer coefficient h for cooling fluid (2.8 per cent Ucon E) and air are respectively given by (in SI units) [**13–16**, **25–29**]

$$h = \begin{cases} 6.960 \times 10^{2}, & \text{if } T \leqslant 404\,\mathrm{K} \\ 2.182 \times 10^{4} - 1.030 \times 10^{2} T + 1.256 \times 10^{-1} T^{2}, & \text{if } 404\,\mathrm{K} < T \leqslant 504\,\mathrm{K} \\ -2.593 \times 10^{4} + 5.500 \times 10^{2} T, & \text{if } 504\,\mathrm{K} < T \leqslant 554\,\mathrm{K} \\ -9.437 \times 10^{4} + 4.715 \times 10^{2} T - 7.286 \times 10^{-1} T^{2} + 3.607 \times 10^{-4} T^{3}, & \text{if } 554\,\mathrm{K} < T \leqslant 804\,\mathrm{K} \\ 1.210 \times 10^{3}, & \text{if } T > 804\,\mathrm{K} \end{cases} \tag{17}$$

$$h_{\mathrm{air}} = \begin{cases} 2.916 + 6.104 \times 10^{-2} T - 1.213 \times 10^{-4} T^{2}, & \text{if } T \leqslant 533\,\mathrm{K} \\ 6.832 + 1.837 \times 10^{-2} T - 1.681 \times 10^{-5} T^{2} + 6.764 \times 10^{-9} T^{3}, & \text{if } 533\,\mathrm{K} < T \leqslant 1200\,\mathrm{K} \\ 3.907 \times 10^{1} - 2.619 \times 10^{-2} T, & \text{if } 1200\,\mathrm{K} < T \leqslant 1311\,\mathrm{K} \\ -2.305 \times 10^{1} + 3.366 \times 10^{-2} T, & \text{if } T > 1311\,\mathrm{K} \end{cases} \tag{18}$$

Finite element method analysis is performed by exploiting axisymmetrical geometry and a single strip is considered for simulations [**9**]. This assumption is employed since the passage of the moving workpiece through the heating and cooling rings promotes a localized phenomenon in this single strip while adjacent material, above and below this strip, is at lower temperatures.

First, a numerical simulation is carried out in order to illustrate the potentiality of the proposed procedure to capture the general thermomechanical behaviour during the quenching process. With this aim, PI hardening of a steel cylinder, of 45 mm diameter and 180 mm length, subjected to an induced layer thickness $e_{\mathrm{PI}} = 3.5$ mm is considered. The specimen induced layer is heated to 1120 K (850 °C) for 5 s and then the surface is sprayed by a liquid medium at 294 K (21 °C) for 10 s [**25**, **26**]. After that, the specimen is subjected to air cooling until a time of 60 s is reached. Figure 1 shows a mesh with 488 nodes and 842 elements employed in numerical simulations after a convergence analysis. The segment OM is at the cylinder centre axis while LK is at the cylinder surface. The null axial displacement condition is imposed in OK and ML in order to consider the restriction associated with adjacent regions of the heated region, which are at lower temperatures. Moreover, longitudinal heat conduction is neglected and thermal boundary conditions impose a convection condition in KL while other faces have adiabatic conditions. Figure 1 also establishes a comparison between experimental results obtained by Camarão [**25**] and those from numerical simulations obtained with the proposed model. Note that results of volumetric fraction of martensite distribution are in close agreement [**13–15**].

The forthcoming analysis considers the effect of local perturbations in the distribution of variables during PI hardening, by introducing a semicircular notch in a long cylindrical steel bar. The cylinder has a notch with radius $r^{*} = 1$ mm and an induced layer thickness, $e_{\mathrm{PI}} = 5$ mm. Figure 2 shows a mesh for $r^{*} = 1$ mm with 503 nodes and 904 elements, which is chosen after a convergence analysis. Similar

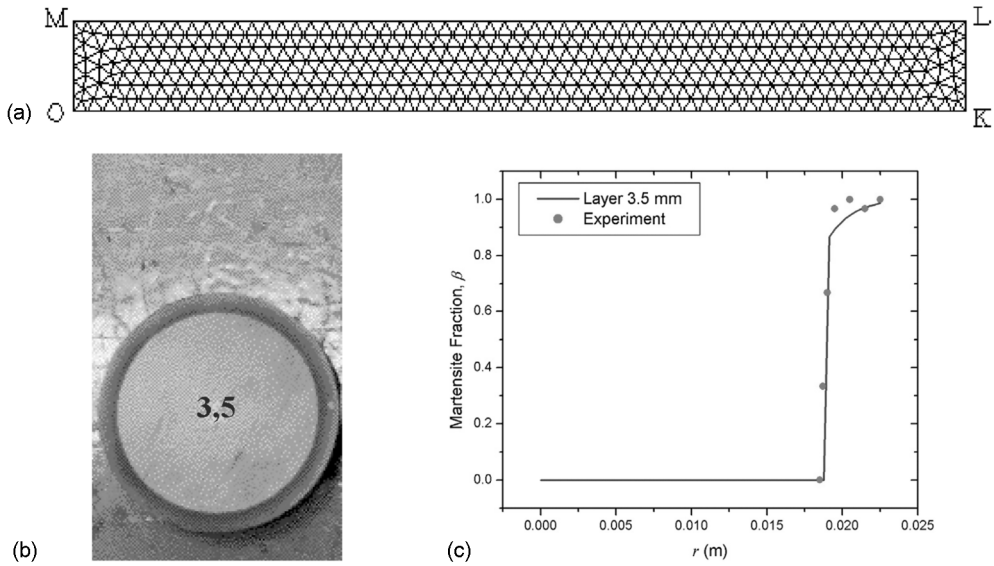

Fig. 1 Comparison between numerical and experimental results: (a) cylinder strip mesh; (b) cross-sections of quenched bar submitted to a 2 per cent Nital etch; (c) volumetric fraction of martensite distribution for $e_{PI} = 3.5$ mm [**13–15**, **25**]

symmetry and boundary conditions of the previous example are considered.

In order to start the analysis of the influence of phase transformation on the prediction of residual stresses, the distribution of the volumetric phase fraction of martensite is considered. Figure 3 presents the volumetric martensite fraction at the final time of the quenching process, showing the phase transformation distribution. Note that phase transformation tends to follow the geometry of the specimen.

The residual stresses generated by the quenching process are now focused on, comparing results predicted by two different models: complete (thermoelastoplastic model with austenite–martensite phase transformation) and without phase transformation (thermoelastoplastic model without phase transformation). Figure 4 shows the radial stresses σ_r, tangential stresses σ_θ, and axial stresses σ_z. Results predicted by the complete model are depicted on the left-hand side of the figure while those predicted by the model without phase transformation are on the right-hand side.

With respect to compressive radial residual stresses, the results predicted by neglecting phase transformation are greater than those considering this effect. The difference of the maximum stress value is about 40 per cent (−378 MPa neglecting phase transformation and −230 MPa for the complete model). On the other hand, considering tensile radial stresses, this difference is greater, about 58 per cent, the values being 455 MPa neglecting phase transformation and 190 MPa considering phase transformation. In contrast with previous results, the predictions of residual tangential stresses σ_θ are underestimated when phase transformations are neglected. The maximum compressive stress values point to a difference of 38 per cent, the values being −736 MPa neglecting phase transformation and −1019 MPa considering phase transformation. Similar results are obtained for tensile stresses that present maximum values of 418 MPa for the model without phase transformation and 485 MPa for the complete model (difference of about 16 per cent). Axial residual stresses σ_z present the same behaviour as the component σ_θ. With

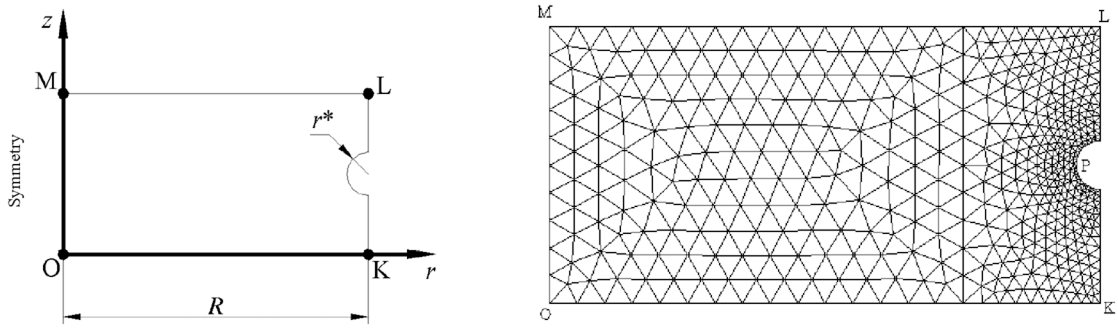

Fig. 2 Cylinder strip with stress concentrator

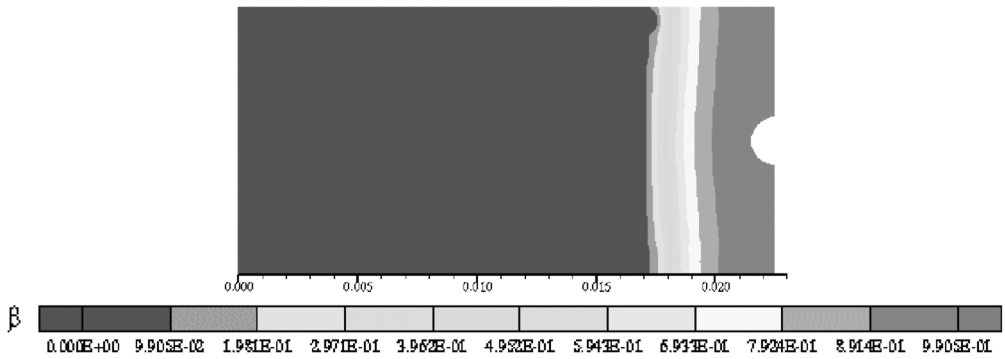

Fig. 3 Volumetric fraction of martensite at the final time

respect to compressive stresses a difference of 74 per cent is observed (−631 MPa neglecting phase transformation and −1095 MPa including phase transformation). On the other hand, tensile stresses may present a difference of about 18 per cent, the values being 547 MPa neglecting phase transformation and 647 MPa for the complete model. With respect to residual shear stress, the analysis shows that the model without phase transformation underestimates the values of the predicted stresses.

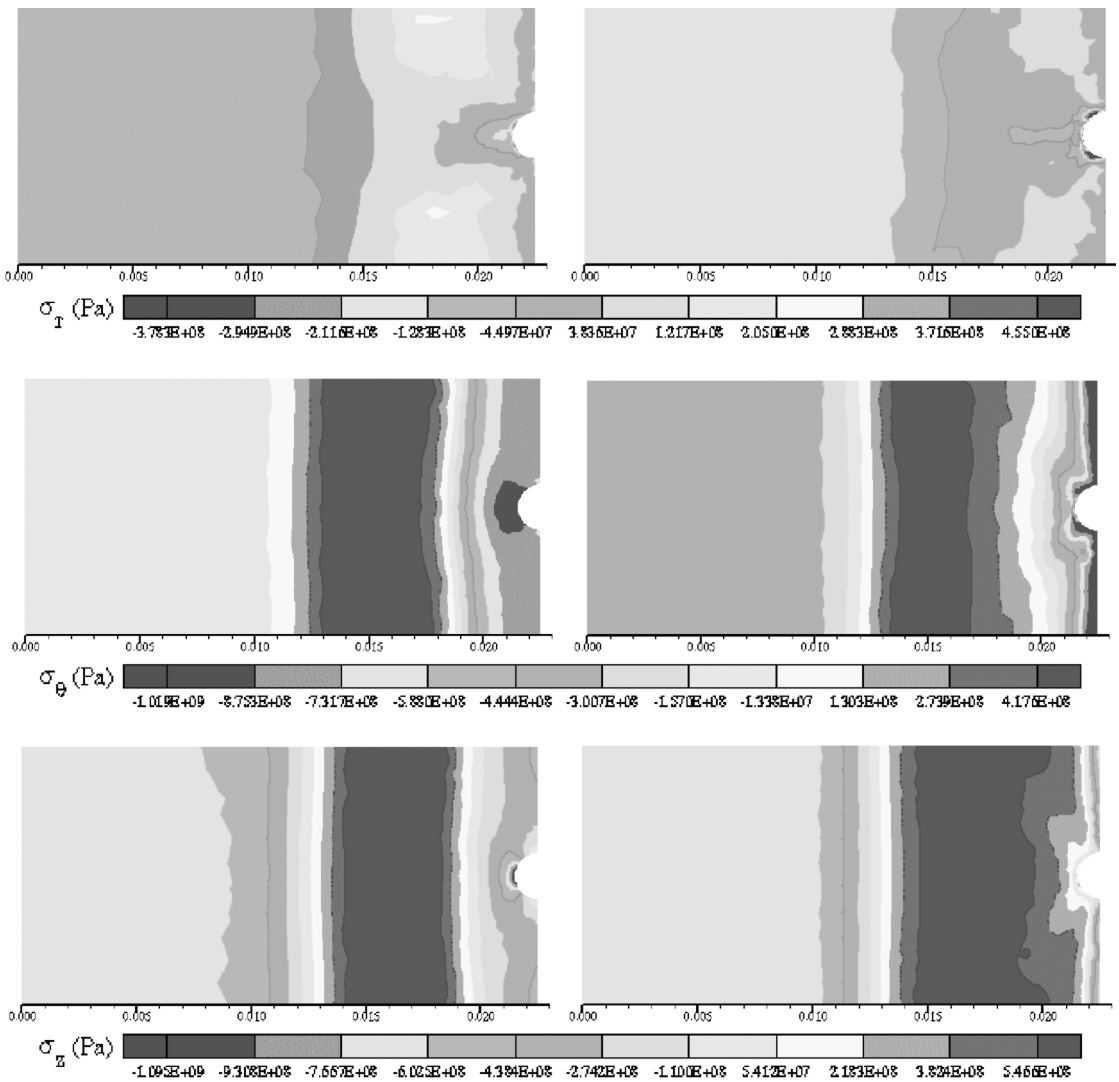

Fig. 4 Residual stresses comparing two different models: complete model (left) and model without phase transformation (right)

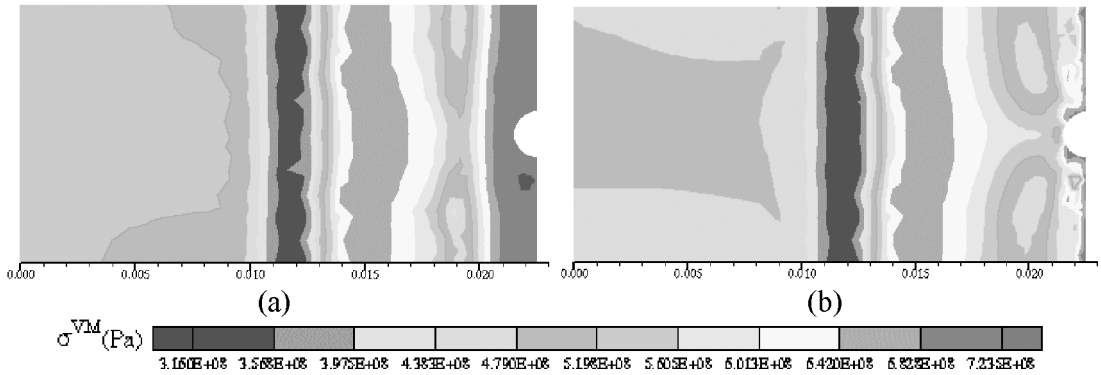

Fig. 5 Von Mises residual stresses: (a) complete model; (b) model without phase transformation

Table 2 Maximum and minimum residual stresses for $r^* = 1.0$ mm comparing two different models: complete and without phase transformation

	σ_r (MPa)	σ_θ (MPa)	σ_z (MPa)	σ_{rz} (MPa)	σ^{vM} (MPa)
Complete					
Minimum	−230	−1019	−1095	−243	+342
Maximum	+190	+485	+647	+240	+724
Without phase transformation					
Minimum	−378	−736	−631	−224	+316
Maximum	+455	+418	+547	+180	+678

The differences between the two models are about 30 per cent (180 MPa neglecting phase transformation and 240 MPa including phase transformation).

An alternative way to evaluate residual stresses generated by the quenching process is to analyse von Mises stresses. With this assumption, note that the model neglecting phase transformation underestimates results when compared with the complete model. This difference is about 7.5 per cent for maximum von Mises stresses. Figure 5 presents the results predicted by both models, pointing out the difference between them. Note that the complete model has a larger critical region.

Table 2 summarizes the previous results, presenting the maximum and minimum values of residual stresses for both models. Note that these values may be related to different points and are presented just for a comparison of the critical points.

Figure 6 presents a comparison between the results predicted by both models, taking data through the periphery of the notch. Note that the complete model predicts compressive values in the entire notch surface, except at the edges where small tensile values are observed. On the other hand, the model without phase transformation predicts tensile stresses in some regions of the notch surface. This can be important data for assessing the structural integrity of a mechanical component subjected to fatigue loadings. Since fatigue cracks usually initiate at the surface and propagate in the presence of tensile stress fields, tensile residual stresses at the surface can be especially critical.

At this point, data through the radius of the cylinder are analysed. Figure 7 presents a comparison between the results predicted by both models, showing that the notch introduces different perturbations in the two models. Note that far from the notch, where phase transformation does not occur, the results predicted by both models are similar. Meanwhile, in the region between node 18 and the cylinder surface, the inclusion of phase transformation causes great discrepancies in the responses of the two models. Again, an important difference that should be pointed out is the variation in the sign of the stress components.

5 CONCLUSIONS

This article presents a comparison between two different models employed to describe the quenching process. The first is a thermoelastoplastic model that includes austenite–martensite phase transformation employing the constitutive model proposed by Pacheco *et al.* [**14**] and Silva *et al.* [**13**]. The second is a thermoelastoplastic model that neglects phase transformation. The finite element method is employed for spatial discretization. A numerical procedure is developed on the basis of the operator split technique associated with an iterative numerical scheme in order to deal with non-linearities of the

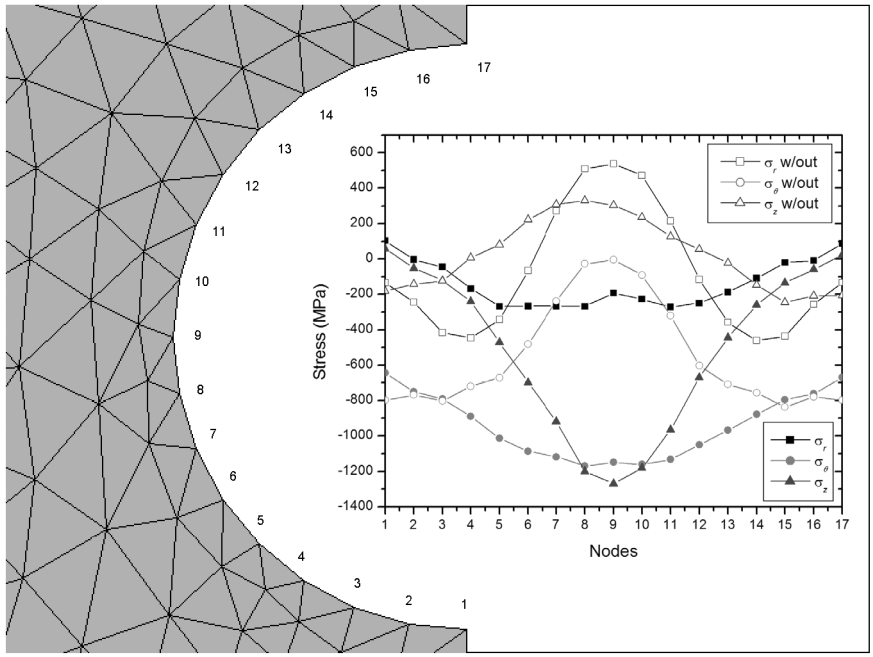

Fig. 6 Residual stresses through the periphery of the notch for both models

formulation. PI hardening of a steel cylindrical body with a semicircular notch is considered. In general, it is possible to conclude that the model neglecting phase transformation underestimates values of residual stresses when compared with results predicted by the model that includes phase transformation. Moreover, differences related to the sign of the residual stresses may be expected between both models. These conclusions point to the necessity of including phase transformations in the

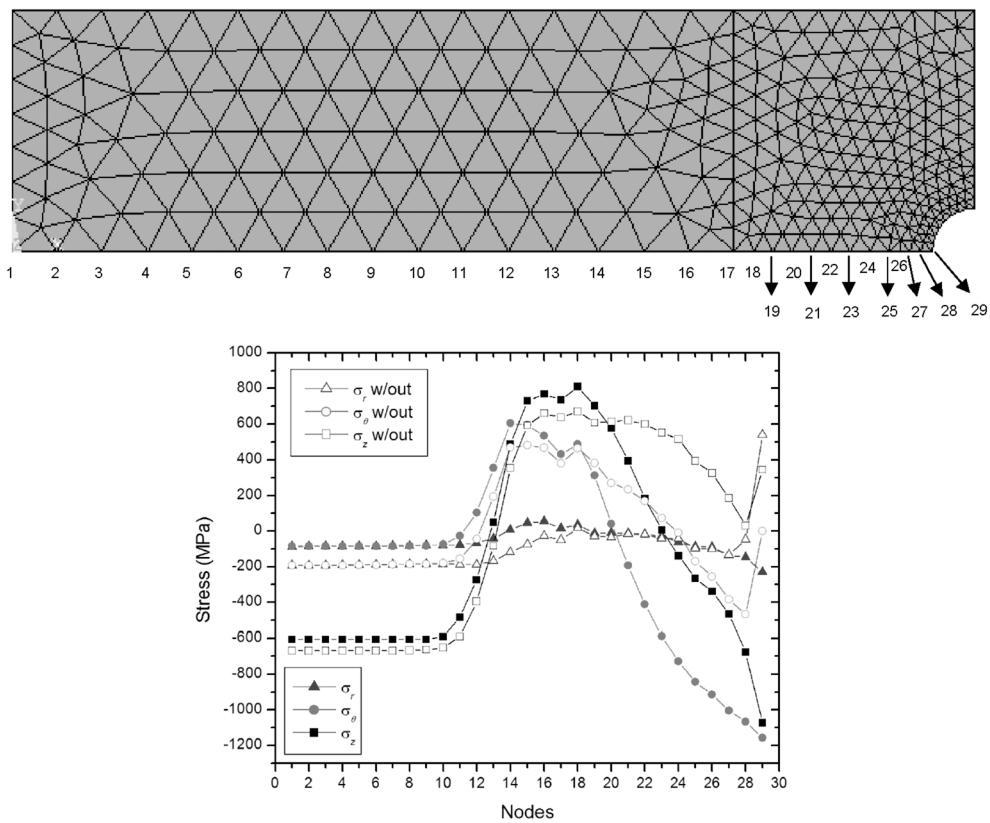

Fig. 7 Residual stresses through the radius of the cylinder for both models

prediction of residual stresses generated by the quenching process.

ACKNOWLEDGEMENTS

The authors would like to acknowledge the support of the Brazilian agencies Conselho Nacional de Desenvolvimento Científico e Tecnológico (CNPq), Coordenação de Aperfeiçoamento de Pessoal de Nível Superior (CAPES), and Fundação de Amparo à Pesquisa do Estado do Rio de Janeiro (FAPERJ).

REFERENCES

1 **Denis, S., Gautier, E., Simon, A.,** and **Beck, G.** Stress–phase-transformation interactions – basic principles, modelling and calculation of internal stresses. *Mater. Sci. Technol.*, October 1985, **1**, 805–814.
2 **Denis, S., Archambault, S., Aubry, C., Mey, A., Louin, J. C.,** and **Simon, A.** Modelling of phase transformation kinetics in steels and coupling with heat treatment residual stress predictions. *J. Physique IV*, September 1999, **9**, 323–332.
3 **Woodard, P. R., Chandrasekar, S.,** and **Yang, H. T. Y.** Analysis of temperature and microstructure in the quenching of steel cylinders. *Metall. Mater. Trans. B*, August 1999, **30**, 815–822.
4 **Sjöström, S.** Interactions and constitutive models for calculating quench stresses in steel. *Mater. Sci. Technol.*, 1985, **1**, 823–829.
5 **Sen, S., Aksakal, B.,** and **Ozel, A.** Transient and residual thermal stresses in quenched cylindrical bodies. *Int. J. Mech. Sci.*, 2000, **42**, 2013–2029.
6 **Çetinel, H., Toparlı, M.,** and **Özsoyller, L.** A finite element based prediction of the microstructural evolution of steels subjected to the tempcore process. *Mechanics Mater.*, 2000, **32**, 339–347.
7 **Gür, C. H.,** and **Tekkaya, A. E.** Numerical investigation of non-homogeneous plastic deformation in quenching process. *Mater. Sci. Engng*, 2001, **A319–A321**, 164–169.
8 **Chen, J. R., Tao, Y. Q.,** and **Wang, H. G.** A study on heat conduction with variable phase transformation composition during quench hardening. *J. Mater. Processing Technol.*, 1997, **63**, 554–558.
9 **Gür, C. H.,** and **Tekkaya, A. E.** Finite element simulation of quench hardening. *Steel Res.*, 1996, **67**(7), 298–306.
10 **Inoue, T.,** and **Wang, Z.** Coupling between stress, temperature, and metallic structures during processes involving phase transformations. *Mater. Sci. Technol.*, 1985, **1**, 845–850.
11 **Denis, S., Sjöström, S.,** and **Simon, A.** Coupled temperature, stress, phase transformation calculation model: numerical illustration of the internal stresses evolution during cooling of a eutectoid carbon steel cylinder. *Metall. Trans. A*, July 1987, **18**, 1203–1212.
12 **Sjöström, S.** Physical, mathematical and numerical modelling for calculation of residual stresses: fundamentals and applications. In Proceedings of the Fourth International Conference on *Residual Stresses*, Baltimore, Maryland, 8–10 June 1994 (in CD format).
13 **Silva, E. P., Pacheco, P. M. C. L.,** and **Savi, M. A.** On the thermo-mechanical coupling in austenite–martensite phase transformation related to the quenching process. *Int. J. Solids Structs*, 2004, **41**(3–4), 1139–1155.
14 **Pacheco, P. M. C. L., Savi, M. A.,** and **Camarão, A. F.** Analysis of residual stresses generated by progressive induction hardening of steel cylinders. *J. Strain Analysis*, 2001, **36**(5), 507–516.
15 **Pacheco, P. M. C. L., Savi, M. A.,** and **Camarão, A. F.** Quenching generated residual stresses in steel cylinders. In Proceedings of the 15th Brazilian Congress on *Mechanical Engineering (ABCM)*, Brazil, 22–26 November 2001 (in CD format).
16 **Silva, E. P.** Modeling and simulation of quenching process in steels using the finite element method (in Portuguese). MSc dissertation, Department of Mechanical Engineering, Instituto Militar de Engenharia (IME).
17 **Ortiz, M., Pinsky, P. M.,** and **Taylor, R. L.** Operator split methods for the numerical solution of the elastoplastic dynamic problem. *Computer Meth. Appl. Mechanics Engng*, 1983, **39**, 137–157.
18 **Lewis, R. W., Morgan, K., Thomas, H. R.,** and **Seethramu, K. N.** *The Finite Element Method in Heat Transfer Analysis*, 1996 (John Wiley, New York).
19 **Gartling, D. K.,** and **Hogan, R. E.** COYOTE – a finite element computer program for nonlinear heat conduction problems. Part I. http://sandia.gov, 1994, Engineering Sciences Center, Sandia National Laboratories (accessed on 12 January 2002).
20 **Segerlind, L. J.** *Applied Finite Element Analysis*, 2nd edition, 1984 (John Wiley, New York).
21 **Ames, W. F.** *Numerical Methods for Partial Differential Equations*, 3rd edition, 1992 (Academic Press, New York).
22 **Nakamura, S.** *Applied Numerical Methods in C*, 1993 (Prentice-Hall, Englewood Cliffs, New Jersey).
23 **Simo, J. C.,** and **Miehe, C.** Associative coupled thermoplasticity at finite strains: formulation, numerical analysis and implementation. *Computer Meth. Appl. Mechanics Engng*, 1992, **98**, 41–104.
24 **Simo, J. C.,** and **Hughes, T. J. R.** *Computational Inelasticity*, 1998 (Springer-Verlag, Berlin, Germany).
25 **Camarão, A. F.** A model to predict residual stresses in the progressive induced quenching of steel cylinders (in Portuguese). PhD thesis, Department of Metallurgical and Materials Engineering, Universidade de São Paulo, São Paulo, Brazil, 1998.
26 **Melander, M.** A computational and experimental investigation of induction and laser hardening. PhD thesis, Department of Mechanical Engineering, Linkoping University, Linkoping, Sweden, 1985.
27 **Hildenwall, B.** Prediction of the residual stresses created during quenching. PhD thesis, Linkoping University, Linkoping, Sweden, 1979.
28 **Camarão, A. F., da Silva, P. S. C. P.,** and **Pacheco, P. M. C. L.** Finite element modeling of thermal and residual stresses induced by steel quenching (in Portuguese). In Seminário de *Fratura, Desgaste e Fadiga de Componentes Automobilísticos*, 2000 (Brazilian Society of Automotive Engineering, Rio de Janeiro) (in CD format).

29 Melander, M. Computer predictions of progressive induction hardening of cylindrical components. *Mater. Sci. Technol.*, October 1985, **1**, 877–882.

APPENDIX

Notation

c	specific heat
C_{ijpq}	auxiliary tensor
e_{PI}	induced layer thickness
E	elastic modulus
E_{A}	elastic modulus for the austenitic phase
E_{ijkl}	elastic tensor
E_{M}	elastic modulus for the martensitic phase
f	yield surface
h	heat transfer coefficient
H	kinematic hardening modulus
H_{ijkl}	kinematic hardening modulus tensor
k	material constant related to martensitic transformation
M_{f}	temperature at which martensite finishes forming in the stress-free state
M_{s}	temperature at which martensite starts to form in the stress-free state
PI	progressive induction
r	radial coordinate
r^*	notch radius
rM_{s}	critical cooling rate for martensite formation
R	cylinder radius
$\mathrm{sgn}(x)$	$= x/\lvert x\rvert$
t	time
T	temperature
T_0	reference temperature
x_i	cartesian coordinate in the i direction
X_{ij}	kinematic hardening tensor
X_{ij}^{d}	deviatoric part of X_{ij}
z	axial coordinate
α_{ij}	kinematic hardening variable tensor
α_T	coefficient of linear thermal expansion
β	volumetric fraction of the martensitic phase
γ	material property related to the total expansion associated with martensitic transformation
$\Gamma(x)$	Heaviside function
δ_{ij}	Kronecker delta
ε_{ij}	total strain tensor
$\varepsilon_{ij}^{\mathrm{p}}$	plastic strain tensor
θ	tangential coordinate
κ	material parameter related to transformation plasticity
λ	plastic multiplier
Λ	coefficient of thermal conductivity
ρ	density
σ_{ij}	stress tensor
σ_{ij}^{d}	deviatoric stress tensor
σ_r	radial stress
σ_{Y}	yield stress
σ_z	axial stress
σ_θ	tangential stress
Φ_{ijpq}	auxiliary tensor
$\dot{}$	$\mathrm{d}(\,)/\mathrm{d}t$